# Application of a digital phase comparator technique to interferometer data

Y. Jiang, D. L. Brower, and L. Zeng
*Electrical Engineering Department and Institute of Plasma and Fusion Research, University of California, Los Angeles, California 90095*

J. Howard
*Plasma Research Laboratory, Research School of Physical Sciences and Engineering, Australian National University, Canberra, A.C.T., Australia*

(Presented on 5 May 1996)

Substantial improvements have been made to increase the frequency bandwidth of the UCLA multichannel interferometer system on TEXT-Upgrade. Recently, a digital phase comparator technique was implemented that has several advantages over the conventional analog phase comparator. The probe and reference wave forms are directly digitized and the phase computed in software using a numerical demodulation algorithm. For the purpose of reducing the data load, aliasing of the laser difference frequency is employed to vary the time response according to experimental demands. © *1997 American Institute of Physics.* [S0034-6748(97)64201-X]

## I. INTRODUCTION

Among the parameters used to evaluate interferometer performance, phase sensitivity, spatial resolution, and temporal resolution are the most important. Phase sensitivity or the minimum detectable phase change depends on the stability of the laser and optical/mechanical system, laser wavelength, and the noise associated with amplifiers, detectors, and phase comparator electronics. Spatial resolution is determined solely by the number and width of chords made available for the measurement. Temporal resolution is limited by the response time of the detectors, amplifiers, and method chosen to evaluate the phase. Improved time resolution for density measurements is desirable in order to allow investigation of plasma instabilities and perturbative transport phenomena (e.g., pellet injection, impurity injection, etc.). Fast plasma instabilities include the sawtooth collapse (30 $\mu$s), tearing modes (50–1000 $\mu$s), and disruptions.

In a heterodyne interferometer system, it is the phase comparator that limits the time response of the measurement. The phase comparator is typically an analog electronic circuit that provides an output voltage proportional to the phase between the reference and plasma legs of the interferometer. Electronic systems are attractive because the comparator output signals require only simple processing, allow for real-time data reduction, and demand only slow sampling rates for digitization and storage. Electronic systems have, however, a sensitivity to noise that results in phase errors and fringes being skipped or added. Unfortunately, the time response of the electronics is often reduced to mitigate this sensitivity to noise thereby further bandwidth limiting the system and removing fast density perturbation information from the output. Analog electronic phase comparators typically operate with 10 kHz bandwidth. Heterodyne far-infrared (FIR) interferometers operate with a difference or intermediate frequency (IF) between the two laser cavities of approximately 1 MHz. In principle, this offers an optimum system time response of 1 $\mu$s. It is the purpose of this article to describe the application of a high-speed phase-comparator technique that allows this optimum response to be realized with reduced phase noise in a flexible, low-cost system readily adaptable to the specific plasma dynamics being addressed. In this approach, the IF frequency is directly digitized and the phase computed via a software-based numerical algorithm. The time response and data load can be tailored to the experimental needs by aliasing the IF frequency while still recovering the desired phase information. The disadvantage of this approach is the computation time required to evaluate the phase.

## II. DEMODULATION TECHNIQUE AND ALIASING

The digitized signal wave form $x(t_n)$ at an IF frequency $\omega_0/2\pi$, whose amplitude and phase are modulated, may be described by

$$x(t_n)=A(t_n)\cos[\omega_0 t_n+\theta(t_n)], \tag{1}$$

where $A(t_n)$ and $\theta(t_n)$ are, respectively, the amplitude and phase modulates at time $t_n=n\Delta t$. This equation may be rewritten as

$$x(t_n)=\tfrac{1}{2}A(t_n)(\exp\{i[\omega_0 t_n+\theta(t_n)]\} + \exp\{-i[\omega_0 t_n+\theta(t_n)]\}). \tag{2}$$

A well known technique for evaluating the phase difference between these two wave forms is digital complex demodulation.[1] In this approach, the phase of the plasma signal is obtained by downshifting the IF frequency as is done in analog demodulation. This is achieved by multiplying Eq. (1) or (2) by $2\exp(-i\omega_0 t_n)$ producing

$$x(t_n)2\exp(-i\omega_0 t_n)=A(t_n)(\exp[i\theta(t_n)] + \exp\{-i[2\omega_0 t_n+\theta(t_n)]\}). \tag{3}$$

A low-pass digital filter is then applied to eliminate the $2\omega_0$ component leaving $y(t_n)=A(t_n)\exp[i\theta(t_n)]$. The phase information is then easily computed as $\theta(t_n)=\tan^{-1}\{\mathrm{Im}[y(t_n)]/\mathrm{Re}[y(t_n)]\}$. In principle, this approach does not require that a reference signal be stored. However, in practice, the IF frequency is not known with perfect precision and may drift during the plasma discharge and, thereby, result in phase errors when downshifting. Consequently, similar analysis must be done on the reference

signal with the plasma phase being defined as the difference between the two, i.e., $\theta_{\text{plasma}}(t_n)=\theta(t_n)-\theta_{\text{ref}}(t_n)$.

The demodulation technique employed in this article differs from digital complex demodulation in that the phase difference between the reference and plasma signals is determined directly.[2] The plasma signal can be expressed in discrete form as

$$x(n)=A(n)\cos[\omega_0' n+\theta(n)], \quad n=0,1,2,\ldots,N-1, \quad (4)$$

where $N$ is the data array length and $\omega_0' = \omega_0 \Delta t$. First, our goal is to generate a complex time domain signal from the real plasma signal. This is accomplished by taking the discrete Fourier transform (DFT) of $x(n)$ giving

$$X(\omega_0')=\frac{1}{N}\sum_{n=0}^{N-1} x(n)e^{-i\omega_0' n}. \quad (5)$$

Taking the inverse DFT at this point would just regenerate Eq. (4). To obtain a complex time domain signal, we now define a new sequence where

$$X^{(1)}(\omega_0')=X(\omega_0'), \quad \text{for } 0\leqslant n\leqslant\frac{N}{2}-1, \quad (6)$$

and

$$X^{(1)}(\omega_0')=0, \quad \text{for } \frac{N}{2}\leqslant n\leqslant N-1. \quad (7)$$

This effectively sets all elements above the Nyquist frequency equal to zero. Now, by taking the inverse DFT, a complex time domain signal is generated, $x^{(1)}(n) \propto \exp\{i[\omega_0' n + \theta(n)]\}$. The exact same procedure is also applied to the reference signal

$$y(n)=B(n)\cos[\omega_0' n+\theta_r(n)], \quad n=0,1,2,\ldots,N-1, \quad (8)$$

yielding a complex time domain signal, $y^{(1)}(n) \propto \exp\{i[\omega_0' n + \theta_r(n)]\}$. If we then multiply the conjugate of the reference by the plasma signal, we arrive at

$$xy^{(1)}(n)=x^{(1)}(n)y^{(1)*}(n)=C(n)\exp\, i[\theta(n)-\theta_r(n)]. \quad (9)$$

The phase difference between the plasma and reference legs is then easily determined from $\theta_{\text{plasma}}=\theta(n)-\theta_r(n) =\tan^{-1}\{\text{Im}[xy^{(1)}(n)]/\text{Re}[xy^{(1)}(n)]\}$. Unlike standard digital complex demodulation, there is no requirement for a low-pass filter because no second harmonic components are produced. This approach actually represents a modified form of digital complex demodulation [see Eq. (2)] where the signal and reference wave forms are reduced to terms proportional to $\exp\{i[\omega_0 t_n+\theta(t_n)]\}$ and $\exp\{i[\omega_0 t_n+\theta_{\text{ref}}(t_n)]\}$, respectively. Here the terms above the Nyquist (i.e., terms with $-i$ in the exponent) have been set to zero. This effectively filters out the $2\omega_0$ component. Now, by multiplying the signal wave form by the complex conjugate of the reference we arrive at a quantity $\propto\exp\{i[\theta(t_n)-\theta_{\text{ref}}(t_n)]\}$ or simply $\propto\exp\{i\,\theta_{\text{plasma}}(t_n)\}$. This modified form of digital complex demodulation can result in improved computing efficiency.

When applying this software-based phase comparator technique, one must be aware of demands being made on the computer system memory and computation time. If the IF frequency is $f_0=1$ MHz and plasma information with time response of 1 $\mu$s is desired, then a total system bandwidth of 2 MHz is required, i.e., data sampling must be such that the Nyquist frequency $f_N\geqslant 2$ MHz. This type of time response may be important for the investigation of fast plasma events like the sawtooth crash. However, for a typical TEXT-Upgrade discharge of 500 ms duration with 15 chords of phase information plus a reference, this would lead to 32 megabytes of memory usage. Fortunately, this type of bandwidth is not typically necessary for most physics investigations. As an example, one way around this problem is to always operate the 10 kHz bandwidth analog phase comparators and utilize the high-speed digital technique for only that portion of the discharge specifically identified for the sawtooth study.

Another approach is to reduce the sampling speed thereby aliasing the IF frequency and reducing the overall system bandwidth. For instance, an 8 $\mu$s time response would require a bandwidth of $f_{\text{bw}}=125$ kHz. This can be achieved by aliasing the IF frequency down to 125 kHz and making $f_N(=f_s/2)=250$ kHz (or $f_s=4\times f_{\text{bw}}$). Hence, by choosing $f_0=875$ kHz and sampling at $f_s=500$ kHz, an aliased IF $f_a=125$ kHz is realized. This would also be the case for $f_0=625$ kHz with the only difference being that the sign of the phase would change. (The IF frequency is chosen to lie in the band $600\leqslant f_0\leqslant 1000$ so that the analog phase comparators can also be used.) Now data for an entire TEXT-Upgrade discharge with 16 channels of information would require two megabytes of memory while the interferometer bandwidth would be increased from 10 to 125 kHz.

When utilizing this approach, it is important to choose $f_0$ such that, when aliased, it lies at approximately $f_N/2$ in order to realize the maximum bandwidth for a given $f_s$. Implicit in the application of the aliasing technique is that the digitizer bandwidth must be sufficient to recover the unaliased signals; otherwise information would be lost. As a practical limit, aliasing the IF below 50 kHz (i.e., $f_s=200$ kHz) is not useful as the IF frequency does shift during the discharge. The IF is tuned remotely between discharges by varying the FIR laser cavity lengths.

## III. APPLICATION TO INTERFEROMETER DATA

For the digital phase comparator technique described in Sec. II, detector output from the reference and plasma legs of the interferometer is directly digitized using a LeCroy 6810 wave form recorder (12 bit) with 5 MHz bandwidth and variable sampling speed up to 5 MHz. The heterodyne multichannel interferometer system is described elsewhere.[3,4] No bandpass filtering was applied to any of the results described below.

In Fig. 1(a), the line-integrated plasma density for a central chord from both the analog and digital phase comparator output is shown. A particularly poor TEXT-Upgrade discharge was chosen where the plasma position control malfunctioned and the plasma was terminated prematurely by a disruption. This provided abrupt dynamic changes in the plasma density that are useful for comparing the phase detection techniques. Both the analog and digital results are seen to be in excellent agreement. For the digital phase com-

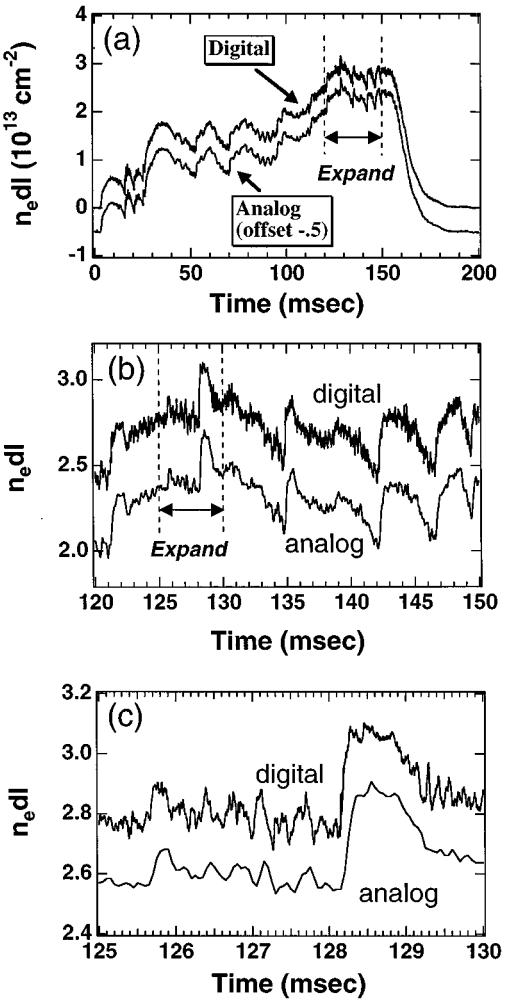


FIG. 1. Line-integrated density from (a) digital and analog phase comparator. (b), (c) Expanded time comparison of digital and analog phase comparator output.

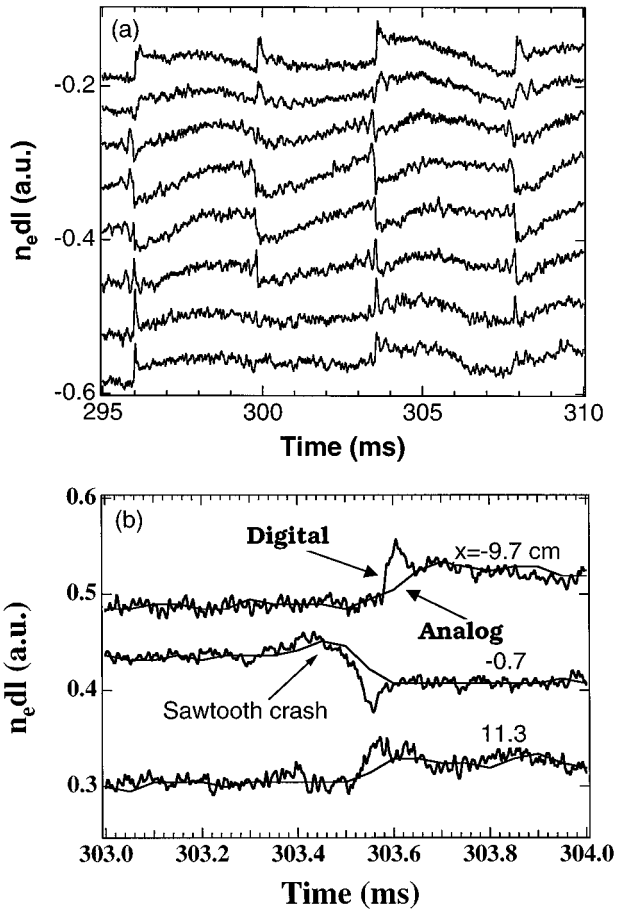


FIG. 2. (a) Digital phase comparator output during sawtooth activity. Chord positions range from −10 (top) to 11 cm (bottom) with 3 cm spacing between chords. (b) Comparison of analog and digital phase comparator output during a sawtooth crash.

parator, the data were sampled at 500 kHz with the IF aliased to 125 kHz. The analog data were sampled at 20 kHz whereas the digital data plot was smoothed by 10.

Expanding the plot about 120 to 150 ms shows that the agreement is still good on a much smaller scale, as shown in Fig. 1(b). The faster time response of the digital technique indicates higher-frequency structures on the density trace. Here, all the digital data points were used. Expanding even further reveals that the fast structures are much more clearly observed on the digital phase comparator [see Fig. 1(c)]. The analog fringe counter either integrates over the fast density changes or misses them completely. A delay of approximately 100 $\mu$s between the digital and analog data is consistent with the 10 kHz bandwidth of the analog system. For the digital system, phase noise on the density trace is $n_e dl \leqslant 10^{11}$ cm$^{-2}$.

In the next example a TEXT-Upgrade discharge with sawtooth activity was chosen. Results from several chords using the digital phase comparator are shown in Fig. 2(a). Note the $m=1$ tearing mode activity immediately prior to and after the sawtooth crash. A clear phase change is observed in the $m=1$ perturbation about the magnetic axis. In Fig. 2(b), three of the channels are expanded and compared with output from the analog phase comparator. The digital phase comparator is able to resolve the sawtooth crash time of approximately 30 $\mu$s. For chords located inside the inversion radius, the crash time varies depending on the position of the $m=1$ precursor. By taking a Fourier transform of the density trace one can generate the spectrum of the high-frequency density fluctuations.

As a final example, the output of the digital phase com-

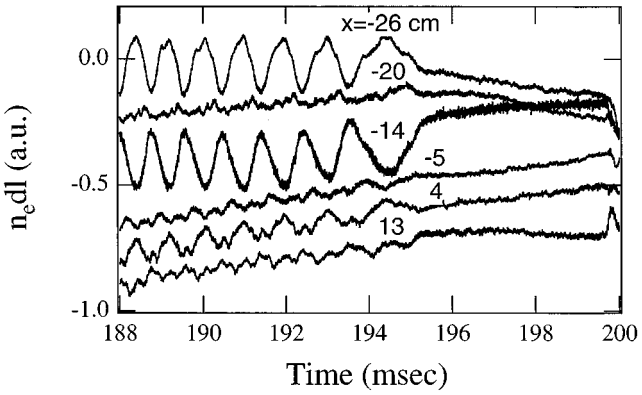


FIG. 3. Digital phase comparator output during tearing mode activity. Note the evidence for higher harmonics on the low-field side.

parator is shown for a TEXT-Upgrade plasma with large-amplitude tearing mode activity as shown in Fig. 3. Large oscillations at a few kHz are observed prior to a locked-mode phase that occurs around 195 ms. Phase changes are observed across the plasma profile with higher harmonics being seen on the low-field side. As in the previous cases, the improved time response of the digital phase comparator allows one to investigate these dynamic plasma responses in greater detail.

## IV. CONCLUSION

In summary, the digital phase comparator technique described in this article is simple and inexpensive to implement when compared to other analog or digital techniques. Code optimization and the use of an array processor represent potentially significant savings of computation time and will be the focus of future development. The digital technique is readily applied to both the interferometer and polarimeter phase data from TEXT-Upgrade.

## ACKNOWLEDGMENT

This research is supported by the U.S. DoE under Grant No. DE-FG03-86ER-53225, Task III.

[1] D. W. Choi, E. J. Powers, R. D. Bengtson, G. Joyce, D. L. Brower, W. A. Peebles, and N. C. Luhmann, Jr., Rev. Sci. Instrum. **57**, 1989 (1986).
[2] J. Howard, Infrared Phys. **34**, 175 (1993).
[3] S. K. Kim, D. L. Brower, W. A. Peebles, and N. C. Luhmann, Jr., Rev. Sci. Instrum. **59**, 1550 (1988).
[4] D. L. Brower, Y. Jiang, W. A. Peebles, S. Burns, and N. C. Luhmann, Jr., Rev. Sci. Instrum. **63**, 4990 (1992).